

## Monovalent Cations Depress the Unfolding of the $\alpha$ -Helical Bacteriorhodopsin at the Air–Water Interface

Akira SHIBATA,\* Junya KOHARA, Satoru UENO, and Takuya YAMASHITA

Faculty of Pharmaceutical Sciences, University of Tokushima, Tokushima 770, Japan.

Received June 29, 1994; accepted September 16, 1994

The structural changes of bacteriorhodopsin (bR) in purple membrane (PM) at the air–water interface and the effects of monovalent cations were examined using a monolayer technique and Fourier transform IR spectroscopy. The low initial coverage ( $c_i$ ) of the interface with PM films significantly caused the denaturation of bR accompanied by a collapse in the PM bilayer structure. The IR spectra of LB films of the PM monolayer films showed that the  $\alpha$ -helical bR molecule in the PM film was partially transformed into a  $\beta$ -sheet depending on the  $c_i$  value. The surface pressure–area ( $\pi$ -A) isotherms of the PM films in the presence of 50 mM alkali metal chlorides were condensed in the sequence  $\text{Cs}^+ > \text{K}^+ > \text{Na}^+ > \text{Li}^+$ . The  $\alpha$ -helix content of bR in the PM films in the presence of 50 mM alkali metal chloride was 84.3% for  $\text{Cs}^+$ , 83.5% for  $\text{K}^+$ , 78.9% for  $\text{Na}^+$ , and 76.0% for  $\text{Li}^+$ , comparable to 68.2%, the value for the subphase ion-free water. The present data indicated that the unfolding of the  $\alpha$ -helical bR in the PM monolayer films was depressed by the addition of small amounts of monovalent cations into the subphase water.

**Keywords** bacteriorhodopsin; monolayer film; structure; stability; monovalent cation; Fourier transform IR

The understanding and control of the structural properties of proteins at the interface is important in a number of fields including adsorption, biomaterial compatibility, interaction with membranes, and molecular recognition.<sup>1–3</sup> Recently, the molecular-order assembling of a functional protein spread at the air–water interface has attracted much attention in relation to the construction of artificial biological systems.<sup>4,5</sup>

The purple membrane (PM) extracted from cultured cells of *Halobacterium halobium* as membrane fragments contains two-dimensionally ordered sheets of bacteriorhodopsin (bR) that use the energy of light to pump protons across the membrane.<sup>6,7</sup> The structural changes in bR during the photocycle is one fundamental aspect of the transport mechanism. The bR molecule in the PM binds divalent cations such as  $\text{Ca}^{2+}$  and  $\text{Mg}^{2+}$ , and these divalent cations interact with negatively charged sites on the surface of the PM through the surface potential and/or through binding by individual ligands.<sup>8,9</sup> Bound divalent cations are partially or completely replaced by treatment with high concentrations of NaCl or KCl. A specific conformation of bR is necessary for at least that part of the cation binding that determines the purple color of the membrane.<sup>9</sup> The replacement of the divalent cations by other ions affects the amplitude of the O photointermediate. The kinetics of the M photointermediate and light-induced  $\text{H}^+$  uptake are not affected by  $\text{Na}^+$  or  $\text{K}^+$ .<sup>8</sup>

The oriented PM films spread at the air–water interface have been employed to study the vectorial photovoltaic responses of bR molecules. Studies for image detection using bR-mounted photovoltaic cells are also in progress using the Langmuir–Blodgett (LB) technique which involves the deposition of PM monolayer films spread at the air–water interface.<sup>10–12</sup> However, the structural stability of protein films spread at this interface, which is an area for the denaturation of proteins, has not been well characterized.<sup>13</sup>

In this paper, we examined the structural stability of bR in the monolayer film of PM fragments at the air–water

interface and the effects of monovalent cations using a monolayer technique and Fourier transform IR (FT-IR) spectroscopy.

### Materials and Methods

PM extracted from cultured cells of *H. halobium* was purified as membrane fragments<sup>14</sup> with a mean diameter of 650 nm which was determined using a Nicomp (Santa Barbara, CA) particle sizer. Salts (LiCl, NaCl, KCl and CsCl) were roasted in an oven at 600 to 700 °C for 7 h to remove any traces of organic compounds. PM films were deposited onto the subphase (pH 5.7) in the absence and the presence of 50 mM salt from an aqueous *N,N*-dimethylformamide (DMF) (25%) suspension under the irradiation of green light. The concentration of PM fragments in the deposition solution was 0.4 mg bR/ml. The validity for the use of DMF has been described elsewhere.<sup>13</sup> The subphase was NANOpure II deionized water (Barnstead Co., Dubuque, IA).

The surface pressure was measured using a computer-controlled trough ( $15 \times 60 \times 1$  cm) attached to a filter-paper Whilhelmy plate hung from the universal tension adapter of a force transducer (Shinkoh, Japan) at  $25 \pm 1$  °C. The interface films were compressed at a speed of 1.0 cm/min ( $1.1 \text{ nm}^2 \text{ bR}^{-1} \text{ min}^{-1}$ ). The PM film was transferred onto a  $\text{CaF}_2$  plate ( $40 \times 20 \times 1$  mm) under a controlled surface pressure of 35 mN/m by the vertical lifting method at a rate of 0.5 cm/min.

Infrared spectra were measured using a Perkin-Elmer (Norwalk, CT) model 1720 FT-IR spectrophotometer equipped with a triglycine sulfate detector with KBr windows at 22 °C. For each spectrum, a 100-scan interferogram was collected in the single beam mode with a  $2 \text{ cm}^{-1}$  resolution. The amide I band contour was fitted with Gaussian/Lorentzian curves. The peak position, bandwidths, intensities, and percent Gaussian–Lorentzian shape are varied to obtain the best fit for the band shapes. The parameters were varied until the residual spectrum obtained by subtraction of the synthetic composite curve from the original data was minimized.<sup>15,16</sup> To determine the content of the secondary structures, the relative areas were estimated from a curve-fit analysis of the spectra.

### Results and Discussion

**PM Films on the Subphase Water** The surface pressure–area ( $\pi$ -A) isotherms for PM films significantly depend on the initial coverage ( $c_i$ ) of the interface with PM films.<sup>13</sup> The  $c_i$  value was defined by dividing the product of the number of bR molecules and the area ( $11.5 \text{ nm}^2$ )<sup>7</sup> per bR molecule in the PM film spread at the interface by the total surface area ( $750 \text{ cm}^2$ ). Typical successive com-

pression–expansion isotherms of the PM film spread at the initial coverage of 0.2 are shown in Fig. 1. After allowing the spread films to stand for 5 min, the compression–expansion was repeated at the same rate between 0 and 40 mN m<sup>-1</sup>. A hysteresis was significantly observed at the beginning of the cycles. As the successive compression–expansion of the PM film was repeated, the isotherms shifted to an increase in area per molecule in the film until a limiting isotherm was finally reached. The limiting molecular area ( $A_0$ ), indicated by extrapolating the surface pressure linear portion of the isotherm below the inflection point to  $\pi=0$ , is plotted against the number of the compression–expansion cycles ( $N_c$ ) (Fig. 1, inset). The limiting area increased with the number of the cycles, and then the final isotherm gave the limiting molecular area ( $A_0$ ) of 58.3 nm<sup>2</sup>/bR denoted by Y in Fig. 1. This value at the initial coverage of 0.2 is too large compared with the cross-sectional area of 11.5 nm<sup>2</sup> per bR molecule in the native PM. Since protein structure is maintained by a balance of forces including those which arise from the hydrophobic effect,<sup>17)</sup> it is expected that any macroscopic structural change of the protein occurs at the interface between high dielectric water and low dielectric air phases. Therefore, the shift to larger value of  $A_0$  may imply the unfolding of bR molecules involving a collapse in the bilayer structure of PM.

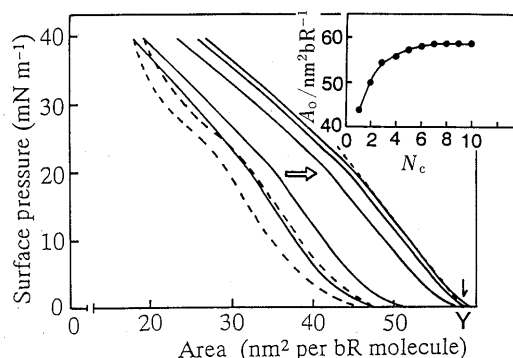


Fig. 1. Successive Compression–Expansion Isotherms of the PM Film Spread at the Initial Coverage of 0.2 and at pH 5.7

Solid lines, compression; dotted lines, expansion. The arrow indicates the direction of the expansion of the isotherms by the successive compression–expansion isotherm. Compression was started after allowing the spread films to stand for 5 min. The inset shows the limiting molecular area ( $A_0$ ) obtained from the compression isotherms depending on the number of the compression–expansion cycles ( $N_c$ ).

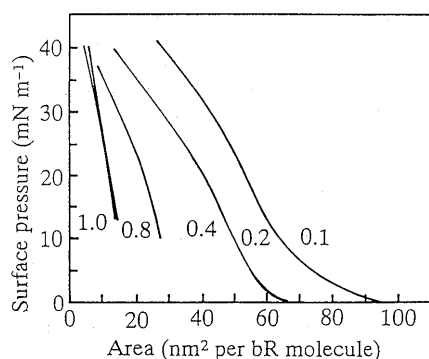


Fig. 2. Surface Pressure–Area Isotherms of PM Films Spread at Different Initial Coverages (0.1, 0.2, 0.4, 0.8, and 1.0) and at pH 5.7

Globular proteins can take various conformations at the air–water interface depending on the initial coverage of the interface with protein.<sup>18)</sup> Figure 2 shows the  $\pi$ -A isotherms of PM films spread at various  $c_i$  values (0.1, 0.2, 0.4, 0.8 and 1.0). The film compression was started after allowing the spread films to stand for 2 h. The spreading of PM fragments at low initial coverage ( $c_i=0.1$  and 0.2) is required for the formation of the monolayered films by lateral diffusion of the PM fragments deposited on the water surface. On the other hand, when the PM suspension was spread onto the subphase water at high initial coverage ( $c_i=0.4, 0.8,$  and 1.0), an increase of the surface pressure of ca. 10 mN m<sup>-1</sup> was observed before the start of film compression. Furthermore, taking into account the agreement of the isotherms between  $c_i=0.8$  and 1.0, the results obtained here imply that the spreading of PM fragments at an initial coverage of more than 0.4 at the interface by the limited surface area described above forces the PM fragments to remain in the water surface as multilayered PM film, and also is disadvantageous for the formation of monolayered (two-dimensional oriented) film. It is possible that the change in the  $\pi$ -A isotherms depending on the initial coverage causes the structural changes of PM at the interface.

The conformational changes in bR resulting from the various initial coverages of the interface with the PM fragments were estimated from the FT-IR spectra. Figure 3 shows the FT-IR spectra of LB films from air-dried PM fragments in the amide I 1700–1600 cm<sup>-1</sup> region transferred onto CaF<sub>2</sub> plates at different initial coverages, together with that of an air-dried PM film cast from a PM aqueous suspension onto a CaF<sub>2</sub> plate. No conformational change in bR due to the contact of the PM fragment with the solid CaF<sub>2</sub> plate was confirmed by comparison of the IR and visible absorption spectra between the cast PM film and PM suspension in water (data not shown). To measure the relative areas of the partially resolved amide I band components, the spectra were curve fit and, as a typical example, the calculated spectrum of the amide I band of the sample prepared at  $c_i=0.4$  is shown in Fig. 4. The curve fitting of the spectrum of bR revealed bands at 1682, 1655 and 1630 cm<sup>-1</sup> in the amide I band region. The fact that the 1655 cm<sup>-1</sup> band is the most prominent supports the finding that the bR molecule is a typical membrane protein having an  $\alpha$ -helical structure.<sup>6)</sup> The bands at 1682 and 1630 cm<sup>-1</sup> are assigned to the  $\beta$ -turn and  $\beta$ -sheet

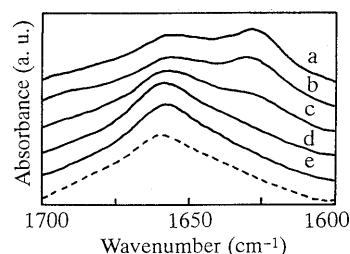


Fig. 3. FTIR Spectra in the Amide I Region of LB Films of bR in the PM Fragments Transferred onto CaF<sub>2</sub> Plates at Different Initial Coverages

Initial coverage: a, 0.1; b, 0.2; c, 0.4; d, 0.8; e, 1.0. The dotted line represents the spectrum of an air-dried PM cast from the PM aqueous suspension onto a CaF<sub>2</sub> plate.

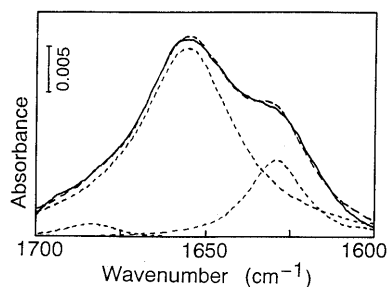


Fig. 4. Observed and Calculated Infrared Spectra in the Amide I Region of LB Film of bR in the PM Prepared at  $c_i=0.4$

Full line, observed; dotted lines, calculated. Dashed line, sum of the individual calculated lines.

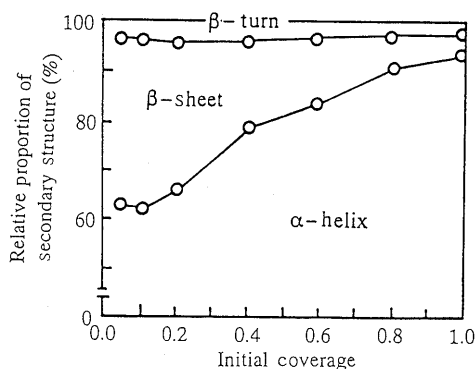


Fig. 5. Relative Proportions of the Secondary Structure of bR in the PM Fragments versus the Initial Coverage

structures, respectively.<sup>16)</sup> The relative proportions of the secondary structure of bR prepared at  $c_i=0.4$  were 78.3% for  $\alpha$ -helix, 17.2% for  $\beta$ -sheet, and 4.5% for  $\beta$ -turn.

Figure 5 shows the relative proportions of the  $\alpha$ -helix,  $\beta$ -sheet and  $\beta$ -turn for the bR molecule as a function of  $c_i$  value. Significant conformational changes of bR were observed for the lower initial coverage of the interface with the PM fragments. An  $\alpha$ -helical bR molecule in the PM fragment was transformed into the  $\beta$ -sheet with a decrease in the initial coverage. For example, the  $\alpha$ -helix content of bR at the initial coverage of 0.2 was about 25% lower than the 92.8% for the native bR which was measured in PM suspension in water. The high initial coverage caused only a slight  $\alpha$ -to- $\beta$  transition in the bR molecule. Little change in the  $\beta$ -turn content was observed. It is difficult to explain why PM fragments unfold at the air-water interface depending on the initial coverage.

The surface pressure of an insoluble monolayer is a function of the water activity at the liquid surface; the existence of a surface tension for liquid water is an indication of a higher molecular free energy and local chemical potential for the interface than for the bulk liquid.<sup>2)</sup> When the PM fragments are deposited onto the water's surface at low initial coverage, the surface active water molecules may cause a disruption of the intra- and intermolecular hydrogen bonds of bR accompanied by a collapse in the PM bilayer structure. The present hypothesis is that the surface active water molecules act as the driving force which displaces the equilibrium in favor of the unfolded structure of the PM, and that the complete denaturation of bR is driven by the thermody-

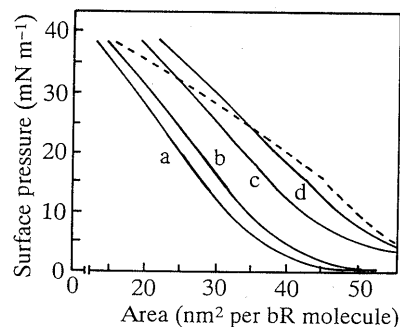


Fig. 6. Surface-Pressure Isotherms of PM Films in the Presence of 50 mM Alkali Metal Chlorides at the Initial Coverage of  $c_i=0.2$  and at pH 5.7

a, CsCl; b, KCl; c, NaCl; d, LiCl. The dotted curve represents the isotherm on the subphase salt-free water.

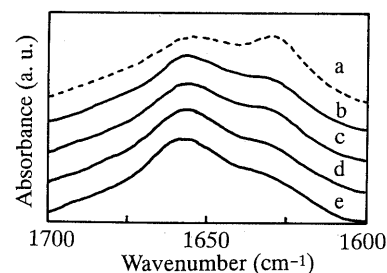


Fig. 7. IR Spectra in the Amide I Region of LB Films of bR in the PM Fragments Prepared in the Presence of 50 mM Salts

a, salt-free; b, LiCl; c, NaCl; d, KCl; e, CsCl.

namic hydrophobic forces acting on the PM.<sup>17)</sup> On the other hand, since the water activity at the interface is lower at the high initial coverage, at which the multilayered PM film may be formed, successive denaturation of bR may become increasingly difficult.

**PM Films on the Subphase Containing Monovalent Cations** A specific conformation of the bR is considered to be necessary for at least part of the cation binding closely correlated to the function of the PM.<sup>9)</sup> Figure 6 shows the  $\pi$ -A isotherms of the PM films in the presence of 50 mM alkali metal chlorides (LiCl, NaCl, KCl and CsCl) at  $c_i=0.2$  and at pH 5.7. The isotherms shifted to a decrease in area per bR molecule in the film due to the presence of salts. The limiting areas per bR molecule in the absence and the presence of 50 mM monovalent cations were 58.3 nm<sup>2</sup> for pure water, 54.8 nm<sup>2</sup> for Li<sup>+</sup>, 48.6 nm<sup>2</sup> for Na<sup>+</sup>, 40.4 nm<sup>2</sup> for K<sup>+</sup>, and 36.6 nm<sup>2</sup> for Cs<sup>+</sup>. The condensing effects of these cations on the PM films are closely related to the stability of bR molecules at the interface.

Figure 7 shows the FT-IR spectra of LB films of the PM fragments in the presence of 50 mM alkali metal chlorides at  $c_i=0.2$ . The amide I band at 1630 cm<sup>-1</sup>, which is revealed in the spectrum of bR obtained on the subphase ion-free water, tends to disappear in the presence of monovalent cations.

The structural stabilization of bR molecules due to these cations was estimated from a curve-fit analysis of the bR spectra in the amide I region. Figure 8 shows the relative proportions of the secondary structure of bR molecules as a function of charge per cross-sectional area of the

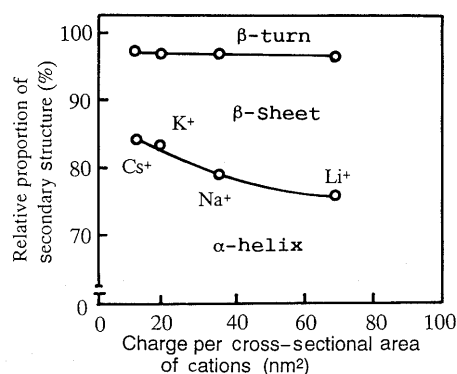


Fig. 8. Relative Proportions of Secondary Structure of bR in the PM Fragments Plotted versus Charge per Cross-Sectional Area of Monovalent Cations

monovalent cations. These charges are smaller for a breaker of the water structure like  $\text{Cs}^+$  than for  $\text{Li}^+$ , a structure maker.<sup>19)</sup> The  $\alpha$ -helix contents of bR in the presence of these cations were 76.0% for  $\text{Li}^+$ , 78.9% for  $\text{Na}^+$ , 83.5% for  $\text{K}^+$ , and 84.3% for  $\text{Cs}^+$ . Compared with the helical content of 68.2% for the bR prepared from the subphase ion-free water, the monovalent cations significantly stabilize the structure of bR in the PM fragments at the interface according to the order of decrease in the charge densities of these ions. The effectiveness of various cations in stabilizing the structure of bR in the PM film at the interface follows the series cesium ion > potassium ion > sodium ion > lithium ion. The dependence of the cation species on the structural stability of bR molecules implies that the Debye-Hückel screening effect of cations does not play a major role. Furthermore, this series is different from the Hofmeister series. The increment of the surface tension of water ( $\Delta\gamma$ ) in the presence of salts decreased in the sequence  $\text{LiCl} > \text{NaCl} > \text{KCl} > \text{CsCl}$ .<sup>19)</sup> A breaker of the water structure like  $\text{Cs}^+$  with small amounts of charge per cross-sectional area is more easily accommodated in the interface than  $\text{Li}^+$ , a structure maker.<sup>20,21)</sup> The bR molecules in PM fragments are oriented with the C-terminal side toward the subphase.<sup>22)</sup> The C-terminal side of bR in the PM composed of amino acids and lipids has ca. 15–18 negative charges per bR.<sup>9)</sup> Hence, the monovalent cations may interact with negatively charged amino acids and lipids by becoming part of the Gouy-Chapman double layer. The present results showed that the electrostatic binding of cations to the negatively charged sites of the C-terminal side of bR in PM film was the major factor responsible for the depression of unfolding of the  $\alpha$ -helical bR molecules at the air-water interface. However, further studies are needed to elucidate the effects of these cations

bound to the C-terminal side of bR in the PM film on the photointermediate and light-induced  $\text{H}^+$  uptake.

### Conclusions

1) The spreading of PM fragments with the lower  $c_i$  at the air-water interface caused significant denaturation of bR accompanied by a collapse of the bilayer structure in the PM. 2) The  $\alpha$ -helical bR molecules in the PM film were partially transformed into the  $\beta$ -sheet depending on the extent of the initial coverage of the interface with the PM fragment. 3) Depression of the unfolding of the  $\alpha$ -helical bR molecules at the interface by monovalent cations was observed; the  $\alpha$ -helix contents of bR in the PM films prepared by the LB technique in the presence of 50 mM alkali metal chlorides were 84.3% for  $\text{Cs}^+$ , 83.5% for  $\text{K}^+$ , 78.9% for  $\text{Na}^+$ , and 76.0% for  $\text{Li}^+$ , and these values were comparable to 68.2%, the value for the subphase ion-free water.

The present studies provide information on the construction of molecular-order assemblies of the functional proteins at the air-water interface.

### References

- 1) T. Yamashita, H. B. Bull, *J. Colloid Interface Sci.*, **27**, 19 (1968).
- 2) L. Ter-Minassian-Saraga, *J. Colloid Interface Sci.*, **80**, 393 (1981).
- 3) H. S. Chan, M. R. Wattenbarger, D. F. Evans, V. A. Bloomfield, K. A. Dill, *J. Chem. Phys.*, **94**, 8542 (1991).
- 4) M. Aizawa, M. Matsuzawa, H. Shinohara, *Thin Solid Films*, **160**, 477 (1988).
- 5) T. Miyasaka, K. Koyama, *Thin Solid Films*, **210/211**, 146 (1992).
- 6) W. Stoeckenius, R. H. Lozier, R. A. Bogomolni, *Biochim. Biophys. Acta*, **505**, 215 (1978).
- 7) S. P. A. Foder, J. B. Ames, R. Gebhard, E. M. M. van der Berg, W. Stoeckenius, J. Lugtenberg, R. A. Mathies, *Biochemistry*, **27**, 7097 (1988).
- 8) C.-H. Chang, J.-G. Chen, R. Govindjee, T. Ebrey, *Proc. Natl. Acad. Sci. U.S.A.*, **82**, 396 (1985).
- 9) C.-H. Chang, R. Jonas, S. Melchiorre, R. Govindjee, T. Ebrey, *Biophys. J.*, **49**, 731 (1986).
- 10) J. Schildkraut, A. Lewis, *Thin Solid Films*, **134**, 13 (1985).
- 11) M. T. Flanagan, *Thin Solid Films*, **99**, 133 (1983).
- 12) T. Miyasaka, K. Koyama, I. Itoh, *Science*, **255**, 342 (1992).
- 13) T. Furuno, H. Sasabe, *J. Colloid Interface Sci.*, **147**, 225 (1991).
- 14) D. Oesterhelt, W. Stoeckenius, *Methods Enzymol.*, **31**, 667 (1974).
- 15) B. R. Singh, M. P. Fuller, G. Schiavo, *Biophys. Chem.*, **36**, 155 (1990).
- 16) A. Dong, P. Huang, W. S. Caughey, *Biochemistry*, **29**, 3303 (1990).
- 17) C. Tanford, *Science*, **200**, 1012 (1978).
- 18) D. J. Adams, M. T. A. Evans, J. R. M. Mitchell, M. C. Phillips, P. M. Rees, *J. Polym. Sci.*, **C34**, 167 (1971).
- 19) J. Ralston, T. W. Healy, *J. Colloid Interface Sci.*, **42**, 629 (1973).
- 20) H. S. Frank, M. W. Evans, *J. Chem. Phys.*, **13**, 507 (1945).
- 21) P. H. Von Hippel, T. Schleich, "Structure and Stability of Biological Macromolecules," ed. by S. Timasheff, G. Fasman, Marcel Dekker, New York, 1969, pp. 417–569.
- 22) S.-B. Hwang, J. I. Korenbrot, W. Stoeckenius, *J. Membr. Biol.*, **36**, 115 (1977).